Published in final edited form as:
*Nature*. 2010 July 1; 466(7302): 128–132. doi:10.1038/nature09143.

# Spatiotemporal regulation of cell-cycle genes by SHORTROOT links patterning and growth

**R. Sozzani**[1,*], **H. Cui**[1,*,†], **M. A. Moreno-Risueno**[1], **W. Busch**[1], **J. M. Van Norman**[1], **T. Vernoux**[1,†], **S. M. Brady**[1], **W. Dewitte**[2], **J. A. H. Murray**[2], and **P. N. Benfey**[1]

[1]Department of Biology and IGSP Center for Systems Biology, Duke University, Durham, North Carolina 27708, USA.

[2]Cardiff School of Biosciences, Biomedical Sciences Building, Cardiff CF10 3AX, Wales, UK.

## Abstract

The development of multicellular organisms relies on the coordinated control of cell divisions leading to proper patterning and growth[1–3]. The molecular mechanisms underlying pattern formation, particularly the regulation of formative cell divisions, remain poorly understood. In *Arabidopsis*, formative divisions generating the root ground tissue are controlled by SHORTROOT (SHR) and SCARECROW (SCR)[4–6]. Here we show, using cell-type-specific transcriptional effects of SHR and SCR combined with data from chromatin immunoprecipitation-based microarray experiments, that SHR regulates the spatiotemporal activation of specific genes involved in cell division. Coincident with the onset of a specific formative division, SHR and SCR directly activate a D-type cyclin; furthermore, altering the expression of this cyclin resulted in formative division defects. Our results indicate that proper pattern formation is achieved through transcriptional regulation of specific cell-cycle genes in a cell-type- and developmental-stage-specific context. Taken together, we provide evidence for a direct link between developmental regulators, specific components of the cell-cycle machinery and organ patterning.

Growth and patterning are key processes that govern the development of multicellular organisms. In some cases, like early *Drosophila* embryogenesis[7], these are independent. However, in many animals and plants, proper development frequently relies on tight coordination of growth and patterning. Disruption of this coordination can lead to unchecked cell growth, resulting in tumorigenesis or misshapen organs[8]. Although the molecular mechanisms involved in pattern formation[9–11] and in cell-cycle control[12–15] have been well



†Present addresses: Department of Biological Science, Florida State University, Florida 32306, USA (H.C.); Laboratoire Reproduction et Développement des Plantes, Université de Lyon, Ecole Normale Supérieure de Lyon, Université Claude Bernard Lyon I, Centre National de la Recherche Scientifique, Institut National de la Recherche Agronomique, cedex 07, Lyon 69364, France (T.V.); Section of Plant Biology and Genome Center, University of California, Davis, California 95616, USA (S.M.B.).
*These authors contributed equally to this work.

**Author Contributions** R.S., M.A.M.-R., J.A.H.M. and P.N.B. conceived and designed the experiments. H.C. and P.N.B. conceived and designed the ChIP-chip experiments. R.S., M.A.M.-R., W.B., J.M.V.N. and W.D. performed the experiments. R.S. and W.B. analysed the data. R.S., H.C., M.A.M.-R., T.V., S.M.B., J.A.H.M. and P.N.B. contributed reagents/materials/analysis tools. R.S., J.M.V.N. and P.N.B. wrote the paper.

**Author Information** The National Center for Biotechnology Information Gene Expression Omnibus (http://www.ncbi.nlm.nih.gov/geo/) accession numbers for the array data discussed in this manuscript are GSE15876 and GSE21338. Reprints and permissions information is available at www.nature.com/reprints. The authors declare no competing financial interests. Readers are welcome to comment on the online version of this article at www.nature.com/nature. Correspondence and requests for materials should be addressed to P.N.B. (philip.benfey@duke.edu).

**Full Methods** and any associated references are available in the online version of the paper at www.nature.com/nature.

**Supplementary Information** is linked to the online version of the paper at www.nature.com/nature.

characterized independently, few connections have been made between the two[16,17]. Here, we identify a new transcriptional regulatory relationship between two key regulators of organ patterning and specific components of the cell-cycle machinery.

SHR and SCR transcription factors control ground tissue patterning by regulating the formative asymmetric division in the immediate progeny of the ground tissue stem cells, known as cortex/endodermis initial (CEI) cells[18,19]. SHR acts non-cell autonomously[20–22] to activate the expression of SCR in the quiescent centre, CEI and endodermis[5, 6, 23,24,25]. To gain insight into the role of the SHR/SCR network in controlling formative cell divisions, we expressed an inducible version of either SHR or SCR in its respective mutant background and characterized the timing of formative divisions after induction.

Before induction, SHR- and SCR-inducible plants had a single mutant ground tissue layer[4,5] (Supplementary Fig. 1). After SHR induction, *SCR* expression was observed within 3 h, indicating that SHR rapidly activates its targets (Supplementary Fig. 1). The first periclinal (parallel to the direction of growth) division in the mutant ground tissue layer occurred 6 h after SHR induction (Fig. 1a, Supplementary Fig. 1 and Supplementary Movie 1) and earlier after SCR induction (Fig. 1b). Two layers of ground tissue with *SCR* expression in the quiescent centre and endodermis (Supplementary Fig. 1), along with a nearly complete Casparian band[5], were detected 24 h after SHR induction (Supplementary Fig. 2). This underlines the combinatorial role of SHR and SCR in regulating formative cell divisions and also indicates that the two inducible systems have slightly different kinetics.

To understand the dynamics of the SHR/SCR regulatory network, we sorted ground tissue cells at several time points after SHR and SCR induction and performed microarray analysis on RNA from the sorted cells[26]. We found 2,478 and 1,903 differentially expressed genes throughout the SHR and SCR time courses, respectively (Fig. 1d, Supplementary Tables 1 and 2). Seven of the eight previously identified SHR direct target genes[24,25] were differentially regulated in the SHR time course (Supplementary Fig. 3) and most of them were also identified in the SCR time course (Supplementary Fig. 3). For both inducible systems, the results for a subset of regulated genes were independently confirmed by quantitative PCR with reverse transcription (RT–qPCR) (Supplementary Fig. 3).

We identified 12 clusters of co-expressed genes downstream of either SHR or SCR (Supplementary Fig. 4). In both SHR and SCR time courses, known SHR targets were found in what we named the 'SCR cluster', as it included *SCR* (Supplementary Fig. 5). Notably, in the SCR-inducible system the expression level of these genes peaked at 3 h as compared to 6 h in the SHR-inducible system. The observed timing of the first formative division followed a similar progression. We therefore propose that genes in the SCR cluster may have a role in regulating formative cell divisions.

In each of the 12 clusters, we identified significantly enriched gene ontology categories (Supplementary Fig. 6, Supplementary Tables 3 and 4). In clusters activated 1 h after SHR (cluster I) and SCR induction (clusters IV and V) (Supplementary Fig. 4), transcription factors were significantly overrepresented. At 6 h after induction and coincident with the onset of formative divisions, gene ontology categories associated with cell-cycle progression and cyclin-dependent protein kinase (CDK) activity were overrepresented in both inducible systems (Supplementary Fig. 6).

To examine the role of the SHR/SCR network in ground tissue formative divisions, we identified genes that were differentially expressed in both inducible systems. In total, 860 genes were regulated by both SHR and SCR (Fig. 1d and Supplementary Table 5). We identified six clusters of co-expressed genes (Supplementary Fig. 7), and gene ontology category enrichment analysis showed predominant molecular functions of these clusters (Fig. 1e and Supplementary

Table 6). Interestingly, one cluster (V) contained genes related to cell division and CDK activity. This indicates that SHR and SCR jointly regulate formative cell divisions by regulating cell-cycle machinery components.

To identify direct and indirect target genes of SHR, we performed chromatin immunoprecipitation-based microarray (ChIP-chip) experiments. We identified 266 genes as direct targets of SHR (Supplementary Table 7). Of these, 65 were differentially expressed in the SHR-inducible system (Fig. 2a and Supplementary Table 8). These genes were positively regulated by SHR and were found primarily in two major expression profiles, with activation at either 1 h or 6 h after SHR induction (Supplementary Fig. 8). The proportion of transcription factor genes was significantly higher than expected by chance (Fig. 2b and Supplementary Table 9), suggesting that SHR directly activates a regulatory cascade involved in several biological processes including cell-cycle progression. Coincident with the onset of periclinal divisions, we identified a D-type cyclin, *CYCD6;1*, that was regulated and whose promoter was directly bound by SHR (Fig. 2c). This gene was one of only six SHR direct target genes in the SCR cluster (Fig. 2d and Supplementary Fig. 9). To confirm direct binding of SHR to the *CYCD6;1* promoter and determine whether SCR also binds this target, we performed ChIP–qPCR. We found significant enrichment for both SHR and SCR binding around 1 kilo-base (kb) upstream of the *CYCD6;1* promoter (Supplementary Fig. 10). The temporal pattern of activation of *CYCD6;1* in the SHR- and SCR-inducible systems, the binding of SHR and SCR to its promoter and the known protein–protein interaction of SHR and SCR[25] support regulation of *CYCD6;1* by both SHR and SCR.

To determine if *CYCD6;1* expression is consistent with a role in the formative division of the immediate progeny of the CEI, the CEI-daughter cell, we generated a transcriptional reporter for *CYCD6;1* (pCYCD6;1::GFP). We observed its expression specifically in CEI/CEI-daughter cells (Fig. 3a); however, we rarely detected expression in all eight CEI/CEI-daughter cells simultaneously, indicating that these formative divisions are not tightly synchronized. In *cycd6;1* mutant seedlings (Supplementary Fig. 11), CEI-daughter cells showed significantly fewer formative divisions (Fig. 3b). Nevertheless, cortical cell number and overall meristem length were comparable to wild type (Supplementary Fig. 12). These results indicate that CYCD6;1 is not required for proliferative cell divisions but is specifically involved in formative divisions needed for proper ground tissue patterning. Because *CYCD6;1* is also expressed in embryonic CEI-daughter cells (Fig. 3a), we examined ground tissue formative divisions during embryogenesis. *cycd6;1* CEI-daughter cells showed significantly fewer periclinal divisions than wild type at both early heart and torpedo embryo stages, whereas all other embryonic root divisions appeared normal (Fig. 3c, d). Interestingly, by the mature embryo stage the number of periclinal divisions in *cycd6;1* and wild-type CEI-daughter cells was more similar (Fig. 3e). We also observed no difference in the seed germination rate between wild type and *cycd6;1* (Supplementary Fig. 13 and Supplementary Movie 2). These results indicate that the *cycd6;1* phenotype is specific to a small number of formative divisions and developmental stages.

Later in root development, *CYCD6;1* expression is restricted to a subset of endodermal cells (Fig. 3f) that undergo a second formative cell division to form middle cortex[27]. In wild type, middle cortex divisions were observed in 52% of roots, as compared to 12% in *cycd6;1* (data not shown). In older plants, expression of pCYCD6;1::GFP was detected in lateral root primordia (Fig. 3g) and pericycle and phloem cells (data not shown). Each of these tissues undergoes formative divisions and all are within the SHR and/or SCR functional domains[17, 24].

Because the *cycd6;1* and *shr* phenotypes are not identical, we proposed that there is functional redundancy in the regulation of this formative division. To test this, we analysed mutations in

*CYCD2;1* and *CYCD5;1*, other D-type cyclins downstream of SHR (Supplementary Table 1). We did not detect abnormal CEI-daughter divisions in either mutant. The double mutants, *cycd6;1cycd2;1* and *cycd6;1cycd5;1* (Supplementary Fig. 14), were not significantly different from *cycd6;1*, suggesting a higher level of functional redundancy, which may include other *CYCD* genes. Taken together, we provide evidence that the SHR/SCR transcriptional network exerts finely tuned control of the formative divisions within the CEI through the restricted spatiotemporal activation of a specific cell-cycle gene.

To identify further genes that participate in this formative division, we profiled transcripts expressed in CEI/CEI-daughter cells by sorting cells from plants containing pCYCD6;1::GFP. Of genes highly expressed in CEI/CEI-daughter cells (Supplementary Table 10), 234 were also differentially regulated in the SHR- and SCR-inducible systems. Notably, 32 showed G2/M-phase-specific expression during cell-cycle progression[28] (Supplementary Fig. 15). On the basis of root-cell-type microarray expression data[29], these mitotic genes are expressed in the same domain as *CYCD6;1* (Fig. 4a), indicating that they are involved in tissue-specific cell divisions. Whether they are involved specifically in formative divisions or more generally in proliferative divisions remains an open question.

Recently, genes involved in formative cell divisions during lateral root formation have been identified[17], 12 of which are regulated by SHR and SCR and expressed in CEI cells (Fig. 4b and Supplementary Table 11). Among these are two CDKs, *CDKB2;1* and *CDKB2;2*, indicating that SHR/SCR regulation of these genes may have a role in formative divisions of ground tissue. To test this hypothesis, we ectopically expressed *CDKB2;1* and *CDKB2;2*, as well as *CYCD6;1*, specifically in the ground tissue. Although root length in these lines was comparable to wild type, we observed extra formative divisions in endodermal cells (Fig. 4c, Supplementary Figs 16 and 17). We also ectopically expressed *CYCD5;1*, *CYCD2;1* and *CYCD1;1* and found no alterations in patterning, indicating that not every D-type cyclin is able to stimulate this formative division (Supplementary Fig. 18). Interestingly, *CDKB2;1* and *CDKB2;2* were not identified as direct targets of SHR, suggesting that they may be regulated by transcription factors activated 1 h after SHR and SCR induction. Taken together, our results indicate that CDKB2;1, CDKB2;2 and CYCD6;1 are involved in specific formative cell divisions downstream of the SHR/SCR network.

To assess whether CYCD6;1 and CDKB2;1 could function independently of SHR in promoting formative divisions, we ectopically expressed them in the *shr* mutant ground tissue. Both CYCD6;1 and CDKB2;1 were able to partially complement the *shr* formative division phenotype (27% and 25% of plants showed divisions, respectively) (Fig. 4d), whereas root length was comparable to *shr-2-J0571* (Fig. 4e). This indicates that these genes have important roles in generating formative divisions downstream of SHR but that there are further genes involved in this process.

We identified a component of the cell-cycle machinery, *CYCD6;1*, as a key SHR/SCR downstream target, providing the first evidence of a direct molecular link between these key developmental regulators and a cell-cycle gene. We further showed that *CYCD6;1* is expressed specifically at the time of the formative cell divisions regulated by SHR/SCR and that altering its expression results in formative division changes in both loss- and gain-of-function plants. Thus, tight spatiotemporal regulation of specific cell-cycle genes is required for proper root pattern formation.

## METHODS SUMMARY

### Plant work

The *Arabidopsis thaliana* ecotypes Columbia (Col-0), Wassilewskija (WS) and C24 were used. Origin and ecotypes are as follows: *shr-2* and pSHR::SHR:GFP *shr-2* (Col-0); pSHR::SHR:GR *shr-2* pSCR::GFP (Col-0); *scr-4* (WS), J0571 enhancer trap (C24). The T-DNA insertion line for (At4g03270) *cycd6;1* is from the GABI-Kat line (GK-368E07).

### Microscopy and phenotypic analyses

To characterize the SHR- and SCR-inducible lines, time-lapse laser scanning confocal microscopy (Zeiss LSM 510) was used. Confocal microscopy was used for observation of embryos and roots of 5- to 15-day-old plants stained with 10 μM propidium iodide. For the *cycd6;1* phenotypic analyses, we counted the number of CEI cells in wild-type and *cycd6;1* mutants and transverse confocal sections were taken just above the quiescent centre cells to determine if the ground tissue formative division had occurred within the CEI daughter.

### Microarray and ChIP-chip analysis

To understand the dynamics of the SHR/SCR regulatory network, we performed time-course microarrays at 0, 1, 3, 6 and 12 h after SHR and SCR induction. Moreover, to examine the transcriptional effects specific to the ground tissue, we sorted the GFP-positive cells from the *J0571* enhancer trap[30] present in both inducible lines. For the SHR/SCR expression time-course microarrays and CEI-specific expression experiments, root tips were dissected at approximately 0.5 cm from the root tip. The protoplasts obtained from these dissected *J0571* or pCYCD6;1::GFP lines were used for fluorescence-activated cell sorting[26]. Two biological replicates were performed for each experiment. Correlations between biological replicates were higher then 0.92 $R^2$.

To determine whether genes regulated by SHR are direct or indirect targets, we performed ChIP-chip. We used the SHR time-course microarray data to determine the detection settings that would allow us to identify SHR direct targets with maximized specificity to sensitivity.

## Supplementary Material

Refer to Web version on PubMed Central for supplementary material.

## Acknowledgments

We thank D. Orlando and R. Twigg for generating the list of probes for the ChIP-array; J. Nieuwland, S. Maughan and C. Collins for construction of the *CYCD6;1* reporter line and assistance in isolation of the *cycd6;1* mutant; L. Sanz, F. Patell and S. Scofield for isolation of the *cycd2;1* and *cycd5;1* mutants; J. Dinneny, M. Noor and members of the Benfey laboratory for their comments on the manuscript. Funding to M.A.M.-R. is provided by the Ministerio de Ciencia y Innovacion (Spain). W.D. and J.A.H.M. were funded by a Biotechnology and Biological Sciences Research Council grant (BB/E022383) and the European Research Area in Plant Genomics network on Plant Stem Cells (BB/E024858). This work was funded by grants to P.N.B. from the NIH (RO1-GM043778 and P50-GM081883) and from the NSF (AT2010 0618304).

## METHODS

## Plant lines and growth conditions

The *Arabidopsis thaliana* ecotypes Columbia (Col-0), Wassilewskija (WS) and C24 were used. Origin and ecotypes are as follows: *shr-2* and pSHR::SHR:GFP *shr-2* (Col-0)[20]; pSHR::SHR:GR *shr-2* pSCR::GFP (Col-0)[24]; *scr-4* (WS)[31]; *J0571* enhancer trap (C24) (http://www.plantsci.cam.ac.uk/Haseloff/Home.html). Transfer DNA insertion lines:

*cycd6;1* (At4g03270) is from the GABI-Kat line described in NASC (GK-368E07); *cycd2;1* (At2g22490) and *cycd5;1* (At4g37630) are from NASC (SALK 049449 and FLAG 148D11, respectively). Primers listed in Supplementary Table 13a were used to verify that *cycd6;1*, *cycd5;1* and *cycd2;1* were homozygous lines. To check *CYCD6;1* expression in *cycd6;1*, the primers listed in Supplementary Table 13b were used.

After surface sterilization using 50% bleach and 0.1% Tween for 5 min and then rinsing three times with sterile water, seeds were stratified at 4 °C for 2 days before being planted on standard media. Seeds were sown and allowed to germinate on vertically positioned Murashige and Skoog agar plates in a Percival incubator with 16 h daily illumination at 22 °C. For the plants grown for the microarray experiments, a layer of nylon mesh (Nitex Cat 03-100/44, Sefar) was added on top of the agar to facilitate transfer onto treatment media and/or root dissection.

## Plasmid construction and plant transformation

Standard molecular biology techniques and the Gateway system (Invitrogen) were used for the cloning procedures. The pSHR::SHR:GR *shr-2-J0571* line was obtained by crossing *shr-2* pSHR::SHR:GR T1 A1/1[24] to the *J0571* enhancer trap line[30]. The pSHR::SHR:GR *shr-2* pSCR::GFP line was obtained by crossing *shr-2* pSHR::SHR:GR T1 A1/1 to the *SCR* reporter (pSCR2.0)[24].To generate pSCR::SCR:GR, pSCR2.0 was used as a promoter region driving the *SCR* coding sequence and glucocorticoid receptor (GR). The pSCR::SCR:GR *scr-4-J0571* line was obtained by transforming pSCR::SCR:GR into *scr-4-J0571* (F4 homozygous lines). Genomic DNA from *Arabidopsis* ecotype Columbia was used as the template for amplification of the upstream regulatory promoter sequence for pCYCD6;1 (2,738 base pairs (bp)) using the cpromCYCD6;1 primers (Supplementary Table 13c) and the PCR product was then cloned into pENTR/D-TOPO. The promoter–reporter pCYCD6;1::GFP:GUS was cloned into the pKGWFS7-Dx destination vector. The coding sequences of *CDKB2;1* (At1g76540), *CDKB2;2* (At1g20930), *SYP111/KNOLLE* (At1g08560), *CYCD1;1* (At1g70210), *CYCD2;1* (At2g22490) and *CYCD5;1* (At4g37630), obtained from The Arabidopsis Information Resource (TAIR)—U12632, U83912, C105142, U60123, U82523 and U66230, respectively —and *CYCD6;1*, were cloned in a pENTR/D-TOPO using the gene coding sequence (cds) amplified with primers as in Supplementary Table 13c. These constructs were then recombined in a two-component system where GAL4 is expressed in the ground tissue (line *J0571*)[30], resulting in expression of the gene of interest, as shown by YFP expression, specifically in the ground tissue. The plasmids were then transformed in the wild-type Col-0 or C24 J0571 enhancer trap by the floral dip method[32].

## Microscopy and phenotypic analyses

The inducible version of either SHR or SCR, expressed in its respective mutant background, was characterized using time-lapse laser scanning confocal microscopy. We morphologically characterized pSHR::SHR:GR *shr-2*-pSCR::GFP, the reporter of which is expressed in the quiescent centre, CEIs and endodermis[24], pSHR::SHR:GR *shr-2-J0571* and the pSCR::SCR:GR *scr-4-J0571* enhancer trap, which specifically marks the ground tissue. Z stacks were taken to locate formative divisions in medial longitudinal sections of SHR- and SCR-induced plants.

Laser scanning confocal microscopy (Zeiss LSM 510) was used to examine embryos and roots of 5- to 15-day-old plants stained with 10 μM propidium iodide.

Fixation, staining and analysis of mature embryos were conducted as described[33].

For the *cycd6;1* phenotypic analyses, we counted the number of CEI cells in wild-type Col-0 ($n$ = 24 and $n$ = 31 of 4- and 5-day-old roots, respectively) and *cycd6;1* mutants ($n$ = 24 and

*n* = 33 of 4- and 5-day-old roots, respectively). Transverse confocal sections were taken just above the quiescent centre cells to determine if formative divisions had occurred in any of the eight CEI-daughter cells. Images of longitudinal confocal sections were analysed to measure the root meristem length and count the number of cortex cells between the quiescent centre and the first elongated cell as described[34].

To analyse middle-cortex formation in wild-type Col-0 and *cycd6;1* roots, Z stacks were taken to locate formative divisions in endodermal cells. The root growth length was assayed by marking the position of the root tips daily on the back of the plate, beginning when the plants were 4 days old. After 4 consecutive days of marking each root (except for roots with the *shr* mutation, for which only 2 days were measured), the plates were scanned and the distance between each mark was assayed using ImageJ software.

Multiple plants (*n* > 50) of individual T3 lines for J0571-UAS::CYCD6;1:YFP (*n* = 4), J0571-UAS::CDKB2;1:YFP (*n* = 2) and J0571-UAS::CDKB2;2:YFP (*n* = 1) were examined and all of these lines showed ectopic formative divisions in the endodermis.

The homozygous line for either J0571-UAS::CYCD6;1:YFP or J0571-UAS::CDKB2;1:YFP was crossed to *shr-2-J0571* homozygous plants. Over-expression of CYCD6;1 or CDKB2;1 was able to partially complement the *shr* formative division phenotype (*n* = 42 and 47, respectively).

Many plants (*n* > 20) of individual T2 lines for J0571-UAS::CYCD1;1:YFP (*n* = 2), J0571-UAS::CYCD2;1:YFP (*n* = 1) and J0571-UAS::CYCD5;1:YFP (*n* = 5) were also examined and none of these lines showed further divisions in the endodermis. Standard error was used and a parametric Student's *t*-test (Figs 3b, 4e) and a non-parametric Wilcoxon test (Fig. 3c–e) were applied for the statistical analysis.

The Casparian band staining was performed on roots from 5- and 7-day-old plants as previously described[24], using 1% agarose sections.

## ChIP–qPCR and ChIP-chip

ChIP was conducted as previously described[25] on roots of 5-day-old seedlings expressing pSHR::SHR:GFP in *shr-2* and pSCR::SCR:GFP in *scr-4*. Immunoprecipitation was performed using a rabbit polyclonal antibody to GFP (ab290, Abcam). For the ChIP–qPCR, enrichment of putative target promoter-region DNA was determined using RT–qPCR and a qPCR efficiency of twofold amplifications per cycle was assumed. Immuno-precipitation from pSHR::SHR:GFP and pSCR::SCR:GFP was compared to mock DNA (bovine serum albumin was used instead of anti-GFP). To assay the *in vivo* binding of SHR and SCR to the promoter region of the *CYCD6;1* gene using ChIP–qPCR, primers were designed to amplify 100–500 bp regions that overlap to span the 4 kb promoter length of the gene. The 500 bp resolution that we obtained in our ChIP–qPCR experiments was owing to technical constraints of primers and materials. The *POLYUBIQUITIN 10* gene (At4g05320) was used to normalize the results between samples (Supplementary Table 13b). Tiling along the *CYCD6;1* promoter region was done using the primers listed in Supplementary Table 13d and was designed to be in ascending order upstream from the *CYCD6;1* ATG. The smaller peak that is visible only in the ChIP–qPCR data could have arisen because of many technical reasons that include variations of material and fixation conditions.

For the genome-wide identification of direct targets of SHR, a ChIP-chip method was developed. First, ChIP was performed on the roots of 5-day-old seedlings expressing the pSHR::SHR:GFP in *shr-2*[25], except that DNA-free protein A agarose beads (Invitrogen) were used. DNA from the ChIP and mock experiments was individually amplified using a random-

primer-based genome amplification method (http://cat.ucsf.edu/pdfs/22_Round_A_B_C_protocol.pdf) with minor modifications. After labelling with Cy3 and Cy5, respectively, following an amino-allyl-dye coupling protocol (http://camd.bio.indiana.edu/files/amino-allyl-protocol.pdf), the DNA was cleaned up using the PCR purification kit (Qiagen) and 3 μg each from the ChIP and mock samples were taken and mixed for hybridization to a custom long oligonucleotide (~60 bases) *Arabidopsis* promoter microarray. The promoter micorarray was fabricated using the Agilent SurePrint technology, and has a capacity of 244,000 features. For each gene in the *Arabidopsis* genome, probes were designed for the intergenic region, the first intron, the 5′ untranslated region and the 3′ untranslated region sequence. The probes were evenly distributed with a density of 125 bp per probe for genes encoding transcription factors and 250 bp per probe for other genes. To identify microRNA gene targets, probes were separately designed for the promoter sequences of about 110 known miRNA genes (http://asrp.cgrb.oregonstate.edu/). Hybridization was performed according to the Agilent ChIP-chip protocol, and images were obtained using an Agilent microarray scanner (model G2565BA) at a resolution of 5 μm. Signal extraction and initial data processing were done using the Agilent feature extraction software. Two biological replicates were conducted.

## Microarray data acquisition and analysis

For the SHR/SCR expression time-course microarrays (at 0, 1, 3, 6 and 12 h after SHR and SCR induction) and CEI-specific expression experiments, root tips were dissected at approximately 0.5 cm from the root tip. The protoplasts obtained from these dissected *J0571* or pCYCD6;1::GFP lines were used for fluorescence-activated cell sorting[26].The GFP-positive sorted cell populations were subsequently frozen before RNA was extracted and used both for RT–qPCR analysis and for microarray analysis using a two-cycle Affymetrix amplification protocol. Total RNA isolation and probes for hybridization were prepared as described[29]. Two biological replicates were performed for each experiment when the correlations between biological replicates were higher than $R^2 = 0.92$. $R^2$ values were as follows: T0_SHR: 1vs.2 (0.950312295); T1_SHR: 1vs.2 (0.972531048); T2_SHR 1vs.2 (0.955786); T3_SHR: 1vs.2 (0.96980011); T4_SHR: 1vs.2 (0.957667748); T0_SCR: 1vs.2 (0.972756742); T1_SCR:1vs.2 (0.955672139); T2_SCR: 1vs.2 (0.972798562); T3_SCR: 1vs.2 (0.922900261); T4_SCR: 1vs.2 (0.976237166); and CEI 1vs2 (0.977861208). A global normalization step was applied to the SHR- and SCR-induction time course using gcRMA. The gcRMA implementation in the Bioconductor and R software packages were used for background correction, quantile normalization and expression-estimate computation (http://www.bioconductor.org)[35]. False-discovery rates were calculated by the significance analysis of microarrays (SAM) algorithm[36]. Differentially expressed genes were identified based on fold-change in expression and a significant *P*-value threshold (twofold change and $P$ value < 0.05). Figure of merit (FOM) led us to identify twelve clusters in both SHR and SCR time courses and six clusters for the common differentially regulated genes. K-means clustering, using a Pearson correlation as the distance metric, was used to group the co-expressed genes downstream of SHR and SCR. For the CEI sorted cell microarrays, mixed model software was used to globally normalize all arrays and to identify differentially expressed probesets[24]. Criteria used to determine enrichment of gene expression in a cell type are as described29. *SCR5* and *J0571* GFP marker lines were excluded from our enrichment analysis because their expression overlapped with the pCYCD6;1::GFP expression domain in the CEIs and CEI-daughter cells. Gene ontology enrichment categories were found using ChipEnrich software[37] (http://www.arexdb.org/software.jsp). Heatmaps were obtained using TMeV freeware (http://www.tm4.org/).

Primers for RT–qPCR on the known targets of SHR were designed to be specific to their coding sequences and are listed in Supplementary Table 13b. As an endogenous control, we used a

gene that did not show differential expression in either SHR or SCR microarrays, At3g52240 (Supplementary Table 13b).

Genes induced by dexamethasone alone were not included in the list of SHR and SCR differentially regulated genes (Supplementary Table 12). The Venn diagrams shown were obtained using VENNY, an interactive tool for comparing lists with Venn Diagrams (http://bioinfogp.cnb.csic.es/tools/venny/index.html). The gene identities were obtained using VirtualPlant 1.0 (http://virtualplant.bio.nyu.edu/cgi-bin/vpweb2/virtualplant.cgi). The expression microarrays and the ChIP-chip data have been deposited in the public functional genomics data repository Gene Expression Omnibus (http://www.ncbi.nlm.nih.gov/geo/).

For ChIP-chip analysis[38], to assess genome-wide binding the processed signal ratios of each experiment were randomly sampled 10,000 times and an empirical *P* value was estimated for each ratio. The empirical *P* values for each probe of the independent ChIP-chip experiments were multiplied. Enrichment was scored by: (1) the length of DNA regions that were covered by probes below a defined *P*-value threshold; (2) a local *P*-value minimum (seed); and (3) the number of nucleotides allowed as gaps within called regions. For each combination of parameters, the detected regions were registered. A gene was assigned to an enriched region if that region was present within 4,000 bp upstream or 300 bp downstream of the transcription start site in an intron, or 300 bp downstream of the gene model. Each parameter combination produced a list of called regions and thus of assigned genes. The proportion of genes that were classified as regulated by SHR (Supplementary Table 1) was recorded for each list. The optimal enrichment detection criteria were defined by those parameters that yielded the highest proportion of SHR-regulated genes and a major fraction of the already described SHR direct genes. These settings were: probe *P*-value seed, $P < 0.0002$; probe *P* value, $P < 0.002$; minimum length of hybridization below *P* value, 210 nucleotides; maximum gap, 195 nucleotides. One-million-fold random sampling of lists containing the same number of genes yielded an empirical *P* value $< 10^{-6}$. The code for the used Python scripts is available on request.

## References


1. Lewis J. From signals to patterns: space, time, and mathematics in developmental biology. Science 2008;322:399–403. [PubMed: 18927385]
2. Herranz H, Milan M. Signalling molecules, growth regulators and cell cycle control in *Drosophila*. Cell Cycle 2008;7:3335–3337. [PubMed: 18948741]
3. Blilou I, et al. The PIN auxin efflux facilitator network controls growth and patterning in *Arabidopsis* roots. Nature 2005;433:39–44. [PubMed: 15635403]
4. Di Laurenzio L, et al. The *SCARECROW* gene regulates an asymmetric cell division that is essential for generating the radial organization of the *Arabidopsis* root. Cell 1996;86:423–433. [PubMed: 8756724]
5. Helariutta Y, et al. The *SHORT-ROOT* gene controls radial patterning of the *Arabidopsis* root through radial signaling. Cell 2000;101:555–567. [PubMed: 10850497]
6. Heidstra R, Welch D, Scheres B. Mosaic analyses using marked activation and deletion clones dissect *Arabidopsis* SCARECROW action in asymmetric cell division. Genes Dev 2004;18:1964–1969. [PubMed: 15314023]
7. Foe VE. Mitotic domains reveal early commitment of cells in *Drosophila* embryos. Development 1989;107:1–22. [PubMed: 2516798]
8. Hartwell LH, Kastan MB. Cell cycle control and cancer. Science 1994;266:1821–1828. [PubMed: 7997877]
9. Schiefelbein J. Cell-fate specification in the epidermis: a common patterning mechanism in the root and shoot. Curr. Opin. Plant Biol 2003;6:74–78. [PubMed: 12495754]
10. Benková E, et al. Local, efflux-dependent auxin gradients as a common module for plant organ formation. Cell 2003;115:591–602. [PubMed: 14651850]

11. Aida M, et al. The PLETHORA genes mediate patterning of the *Arabidopsis* root stem cell niche. Cell 2004;119:109–120. [PubMed: 15454085]
12. Wu L, et al. The E2F1–3 transcription factors are essential for cellular proliferation. Nature 2001;414:457–462. [PubMed: 11719808]
13. Blilou I, et al. The *Arabidopsis HOBBIT* gene encodes a CDC27 homolog that links the plant cell cycle to progression of cell differentiation. Genes Dev 2002;16:2566–2575. [PubMed: 12368267]
14. Andersen SU, et al. Requirement of B2-type cyclin-dependent kinases for meristem integrity in *Arabidopsis thaliana*. Plant Cell 2008;20:88–100. [PubMed: 18223038]
15. Ebel C, Mariconti L, Gruissem W. Plant retinoblastoma homologues control nuclear proliferation in the female gametophyte. Nature 2004;429:776–780. [PubMed: 15201912]
16. Weigmann K, Cohen SM, Lehner CF. Cell cycle progression, growth and patterning in imaginal discs despite inhibition of cell division after inactivation of *Drosophila* Cdc2 kinase. Development 1997;124:3555–3563. [PubMed: 9342048]
17. De Smet I, et al. Receptor-like kinase ACR4 restricts formative cell divisions in the *Arabidopsis* root. Science 2008;322:594–597. [PubMed: 18948541]
18. Benfey PN, et al. Root development in *Arabidopsis*: four mutants with dramatically altered root morphogenesis. Development 1993;119:57–70. [PubMed: 8275864]
19. Pysh LD, Wysocka-Diller JW, Camilleri C, Bouchez D, Benfey PN. The GRAS gene family in *Arabidopsis*: sequence characterization and basic expression analysis of the *SCARECROW-LIKE* genes. Plant J 1999;18:111–119. [PubMed: 10341448]
20. Nakajima K, Sena G, Nawy T, Benfey PN. Intercellular movement of the putative transcription factor SHR in root patterning. Nature 2001;413:307–311. [PubMed: 11565032]
21. Gallagher KL, Paquette AJ, Nakajima K, Benfey PN. Mechanisms regulating SHORT-ROOT intercellular movement. Curr. Biol 2004;14:1847–1851. [PubMed: 15498493]
22. Gallagher KL, Benfey PN. Both the conserved GRAS domain and nuclear localization are required for SHORT-ROOT movement. Plant J 2009;57:785–797. [PubMed: 19000160]
23. Sabatini S, Heidstra R, Wildwater M, Scheres B. SCARECROW is involved in positioning the stem cell niche in the *Arabidopsis* root meristem. Genes Dev 2003;17:354–358. [PubMed: 12569126]
24. Levesque MP, et al. Whole-genome analysis of the SHORT-ROOT developmental pathway in *Arabidopsis*. PLoS Biol 2006;4:e143. doi:10.1371/ journal.pbio.0040143. [PubMed: 16640459]
25. Cui H, et al. An evolutionarily conserved mechanism delimiting SHR movement defines a single layer of endodermis in plants. Science 2007;316:421–425. [PubMed: 17446396]
26. Birnbaum K, et al. A gene expression map of the *Arabidopsis* root. Science 2003;302:1956–1960. [PubMed: 14671301]
27. Paquette AJ, Benfey PN. Maturation of the ground tissue of the root is regulated by gibberellin and *SCARECROW* and requires *SHORT-ROOT*. Plant Physiol 2005;138:636–640. [PubMed: 15955927]
28. Menges M, de Jager SM, Gruissem W, Murray JA. Global analysis of the core cell cycle regulators of *Arabidopsis* identifies novel genes, reveals multiple and highly specific profiles of expression and provides a coherent model for plant cell cycle control. Plant J 2005;41:546–566. [PubMed: 15686519]
29. Brady SM, et al. A high-resolution root spatiotemporal map reveals dominant expression patterns. Science 2007;318:801–806. [PubMed: 17975066]
30. Haseloff J. GFP variants for multispectral imaging of living cells. Methods Cell Biol 1998;58:139–151. [PubMed: 9891379]
31. Fukaki H, et al. Genetic evidence that the endodermis is essential for shoot gravitropism in *Arabidopsis thaliana*. Plant J 1998;14:425–430. [PubMed: 9670559]
32. Clough SJ, Bent AF. Floral dip: a simplified method for Agrobacterium-mediated transformation of *Arabidopsis thaliana*. Plant J 1998;16:735–743. [PubMed: 10069079]
33. Bougourd S, Marrison J, Haseloff J. Technical advance: an aniline blue staining procedure for confocal microscopy and 3D imaging of normal and perturbed cellular phenotypes in mature *Arabidopsis* embryos. Plant J 2000;24:543–550. [PubMed: 11115135]
34. Casamitjana-Martinez E, et al. Root-specific CLE19 overexpression and the sol1/2 suppressors implicate a CLV-like pathway in the control of Arabidopsis root meristem maintenance. Curr. Biol 2003;13:1435–1441. [PubMed: 12932329]

35. Gentleman RC, et al. Bioconductor: open software development for computational biology and bioinformatics. Genome Biol 2004;5:R80. [PubMed: 15461798]

36. Tusher VG, Tibshirani R, Chu G. Significance analysis of microarrays applied to the ionizing radiation response. Proc. Natl Acad. Sci. USA 2001;98:5116–5121. [PubMed: 11309499]

37. Orlando DA, Brady SM, Koch JD, Dinneny JR, Benfey PN. Manipulating large scale Arabidopsis microarray expression data: identifying dominant expression patterns and biological process enrichment. Methods Mol. Biol 2009;553:57–77. [PubMed: 19588101]

38. Busch W, et al. Transcriptional control of a plant stem cell niche. Dev. Cell 2010;18:849–861. [PubMed: 20493817]

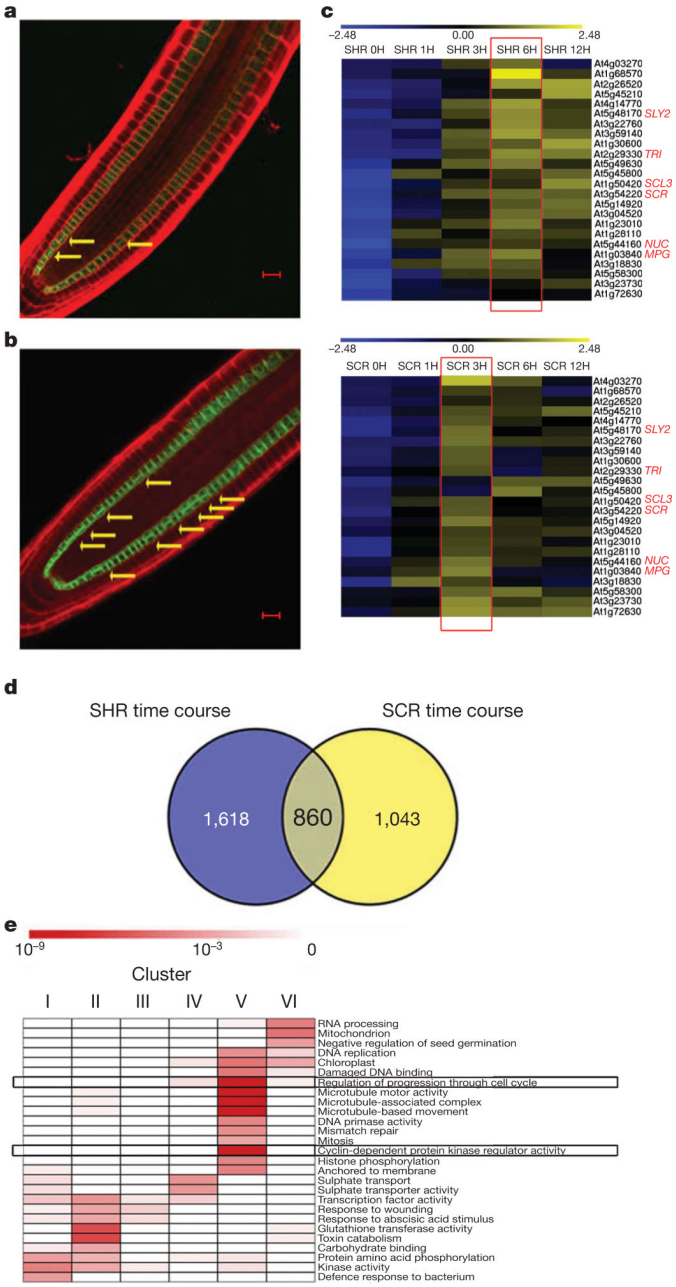


**Figure 1. SHR and SCR regulate genes involved in formative cell divisions**

**a, b**, Median longitudinal root sections from 5-day-old seedlings 6 h after induction of pSHR::SHR:GR in *shr-2-J0571* (**a**) and of pSCR::SCR:GR in *scr-4-J0571* (**b**). Arrows indicate formative divisions. Scale bars, 20 μm. **c**, Heatmap of genes in the SCR cluster as expressed in SHR-inducible (top) and SCR-inducible systems (bottom). Yellow, upregulation; blue, downregulation. Red boxes indicate gene expression peaks; red text shows known SHR targets. **d**, Venn diagram of significant genes in SHR- and SCR-inducible systems. **e**, Gene ontology category enrichment of SHR and SCR common genes. Black boxes indicate cell-cycle regulation gene ontology categories.

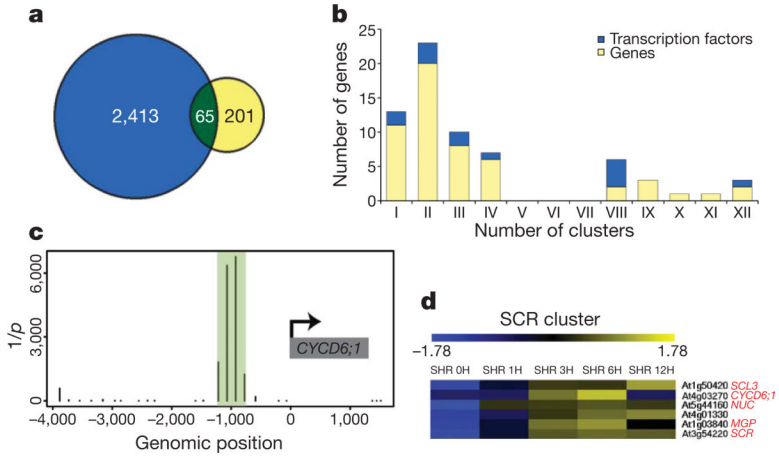


**Figure 2. SHR directly activates transcription factors and a cell-cycle gene**

**a**, Venn diagram of genes in SHR time course and SHR direct targets. **b**, Bar graph of SHR direct-target genes as distributed within the 12 clusters of SHR induced genes. The blue portion indicates the number of transcription factors. **c**, Binding profile of SHR to the upstream regulatory region of *CYCD6;1*, as determined by ChIP-chip. Inverted *P* values for enrichment (*y* axis) at genomic positions relative to the transcriptional start site (TSS) of the primary mRNA (*x* axis). Green-shaded area, region detected as enriched. **d**, Heatmap representation of the six direct targets activated 6 h after SHR induction.

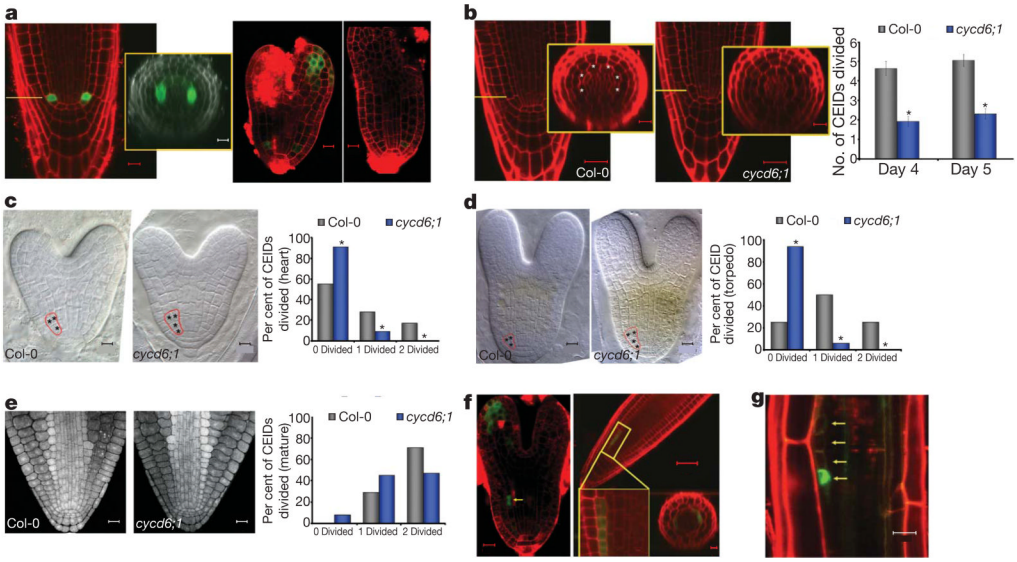


**Figure 3. Spatiotemporal activation of *CYCD6;1***

**a**, pCYCD6;1::GFP expression in CEI/CEI-daughter cells of 5-day-old roots (left), heart (middle) and torpedo (right) embryos. Inset, cross-section. Scale bars, 10 μm. **b**, Five-day-old Col-0 (left) and *cycd6;1* mutant (right). Scale bars, 20 μm. Insets, cross-sections (scale bars, 10 μm). Bar graph of divided CEI-daughter cells (CEIDs) in 4- and 5-day-old wild-type and *cycd6;1* seedlings ($n$ = 24 and 31). **c–e**, Heart, torpedo and mature wild-type and *cycd6;1* embryos with bar graphs ($n$ = 58, 40 and 35). Scale bars, 10 μm(**c, d**), 20 μm (**e**). **f**, pCYCD6;1::GFP in late torpedo embryo (left; scale bar, 10 μm) and 10-day-old root (right; scale bar, 50 μm). Inset, magnification (left); cross-section (right; scale bar, 10 μm). **g**, Fifteen-day-old root. Arrows indicate lateral root primordium. Scale bar, 20 μm. Asterisks show statistical significance ($P < 0.001$). Error bars are s.e.m.

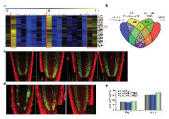

**Figure 4. SHR and SCR activate cell-cycle genes for formative divisions**

**a**, Heatmap showing expression of mitotic genes downstream of SHR/SCR in cell types. Red boxes highlight high expression. **b**, Venn diagram of genes from four data sets. Grey region, genes involved in formative divisions downstream of SHR/SCR. **c**, Seven-day-old roots, from left to right: with *J0571*; J0571-UAS::CYCD6;1:YFP (*n* = 53); J0571-UAS::CDKB2;1:YFP (*n* = 53); and with J0571-UAS::CDKB2;2:YFP (*n* = 28). Scale bars, 10 μm. **d**, 7-day-old roots, from left to right: with *shr-2-J0571; shr-2* with J0571-UAS::CYCD6;1:YFP (*n* = 42); and with J0571-UAS::CDKB2;1:YFP (*n* = 47). Scale bars, 10 μm. Insets, YFP-tagged proteins. Asterisks show formative divisions. **e**, Bar graph of root of 4- and 5-day-old plants, as in **c** and **d** (*n* = 21 each). Error bars are s.e.m.